ELSEVIER

Marine Chemistry 50 (1995) 189–206

MARINE CHEMISTRY

Iron uptake and growth limitation in oceanic and coastal phytoplankton

William G. Sunda, Susan A. Huntsman

Beaufort Laboratory, National Marine Fisheries Service, NOAA, Beaufort, NC 28516, USA

Received 9 July 1994; accepted 23 January 1995

Abstract

Iron concentrations in open ocean are orders of magnitude lower than levels in coastal waters. Experiments with coastal and oceanic phytoplankton clones representing different algal groups and cell sizes indicate that cellular iron uptake rates are similar among the species when rates are normalized to cell surface area. This similarity in rates apparently is explained by evolutionary pressures that have pushed iron uptake in all species toward the maximum limits imposed by diffusion and ligand exchange kinetics. Because of these physical/chemical limits on uptake, oceanic species have been forced to decrease their cell size and/or to reduce their growth requirements for cellular iron by up to 8-fold. The biochemical mechanisms responsible for this reduction in metabolic requirements are unknown.

1. Introduction

Despite being the fourth most abundant element in the Earth's crust, iron is present at subnanomolar concentrations in most near-surface oceanic waters due to the insolubility of Fe(III) oxides and hydroxides, efficient scavenging by particle surfaces, and uptake by phytoplankton (Martin and Gordon, 1988; Martin et al., 1989,1990a,b, 1993). Iron is important in plant metabolism where it is required for photosynthetic and respiratory electron transport, nitrate reduction, chlorophyll synthesis, and detoxification of reactive oxygen species. Results of iron enrichment experiments in bottles provide evidence that low iron abundance limits productivity and controls species diversity in many oceanic algal communities, particularly those in upwelling regions (Martin et al., 1989,1991). Recently, the addition of iron to a 64 km^2 patch of the equatorial Pacific Ocean increased phytoplankton productivity by 3-fold, confirming the iron limitation hypothesis (Martin et al., 1994).

Iron occurs at 100 to 1000 times higher concentrations in coastal waters, and culture experiments show that iron requirements of oceanic and coastal species reflect this neritic/oceanic difference, i.e. oceanic clones are able to grow at much lower iron concentrations than their neritic counterparts (Brand et al., 1983). In a previous study we conducted with a pair of neritic and oceanic diatoms, the oceanic species, *Thalassiosira oceanica*, had a much lower growth requirement for cellular iron than its coastal congener, *T. pseudonana*, but the iron uptake rates of the two species were similar (Sunda et al., 1991). Thus, the ability of the oceanic species to outgrow its neritic congener at low iron concentrations was due almost entirely to its unusually low cellular iron requirement.

In the present study, we investigated the wider

Elsevier Science B.V.
SSDI 0003-2670(95)00035-6

applicability of the above results by measuring relationships among external iron concentration, iron uptake rates, cellular iron concentrations, chlorophyll *a*, mean cell size and growth rate for the same two species (*T. pseudonana*, clone 3H, and *T. oceanica*, clone 13-1) and four additional oceanic and coastal isolates. The oceanic isolates included *Emiliania huxleyi* (clone A1387), a coccolithophore from the Gulf of Mexico, and *Pelagomonas calceolata* (clone MC-1), a small flagellate from the North Pacific gyre. The two coastal isolates were the diatom *Thalassiosira weissflogii* (Actin) and the dinoflagellate *Prorocentrum minimum* (Exuv), both isolated from estuaries on Long Island. In addition to representing a diversity of habitats and algal classes, the six isolates also represented a range in cell diameter, a critical factor regulating nutrient uptake dynamics. Cell diameters were ~ 2 μm for *P. calceolata*, 3 μm for *E. huxleyi*, 4 μm for *T. pseudonana*, 5–6 μm for *T. oceanica*, ~ 12 μm for *T. weissflogii*, and ~ 13 μm for *P. minimum*.

2. Experimental

Long-term growth and iron uptake experiments were conducted in EDTA/metal ion buffered seawater media, utilizing the same or similar methods as in our previous iron study with *T. pseudonana* and *T. oceanica* (Sunda et al., 1991). Cells were grown at 20°C and pH 8.1–8.2 in 450 ml polycarbonate bottles containing 200 ml of seawater ($S = 36$) medium. They were grown under fluorescent lighting (VITA-LITE; Duro Test Corp.) at 500 μmol quanta m^{-2} s^{-1} PAR provided on a 14:10 h light:dark cycle. In two experiments, the light intensity was reduced to 175 μmol quanta m^{-2} s^{-1} by use of neutral density light filters.

The experimental seawater was prepared from filtered (0.4 μm), Gulf Stream water enriched with 32 μM $NaNO_3$, 2 μM Na_2HPO_4, 40 μM Na_2SiO_3, 10nM Na_2SeO_3, 0.1 μg l^{-1} vitamin B_{12}, 0.1 μg l^{-1} biotin, and 20 μg l^{-1} thiamin. In one experiment with *E. huxleyi*, 32 μM NH_4Cl was added as a nitrogen source instead of nitrate. The major nutrient stock solutions were treated with precleaned Chelex resin to remove trace metal contaminants (Price et al., 1988/1989). The media also received additions of trace metal ion buffer systems to regulate and quantify the free ion concentrations of iron and other trace metal nutrients. These buffers consisted of 0.1 mM EDTA, 50 nM $MnCl_2$, 40 nM $CuCl_2$, 100 nM $ZnCl_2$, 40 nM $CoCl_2$, 100 nM $NiCl_2$, and various concentrations of $FeCl_3$ radiolabeled with ^{55}Fe or ^{59}Fe. After preparation, the media were equilibrated for 24 h before inoculation of cells.

Previous research with the diatom *T. weissflogii* and a coastal coccolithophore and has shown that the uptake of iron is determined by the concentration of dissolved inorganic Fe(III) species [$Fe(OH)_2^+$ and $Fe(OH)_4^-$] (Hudson and Morel, 1990). Mean concentrations of dissolved inorganic iron, [Fe′], in our experiments were computed from measurements of iron complexation to EDTA in model seawater systems in both the dark and the light. These measurements involved reaction of labile inorganic iron species with 8-hydroxyquinoline preadsorbed onto C_{18}-SEP-PAK cartridges. They are described in detail in another paper (Sunda and Huntsman, in prep.). The measurements indicated that at the mean pH of our experiments (8.16), the ratio of dissolved inorganic iron to iron-EDTA chelates is 0.00119 in the dark and 0.0020 and 0.0035, respectively, at light intensities of 175 and 500 μmol quanta m^{-2} s^{-1} PAR. These values yield weighted mean ratios of 0.00166 and 0.0025 at the lower and higher light intensities, respectively, over a 14:10 h light:dark cycle. Values for [Fe′] were computed by multiplying these weighted averages by the total iron concentration. Due to precipitation of iron hydroxide, these values could only be computed for total Fe concentrations ≤ 300 nM ([Fe′] ≤ 0.7 nM).

Total iron concentration was computed from the sum of the concentration of added $FeCl_3$, the background iron concentration, and iron added with the radiotracer and EDTA stock solutions. Background iron in the medium without EDTA (0.7 nM) was measured by furnace atomic absorption spectrometry (FAAS) following Co/APDC extraction (Boyle, 1977; Hanson and Quinn, 1983). Iron in the EDTA and nutrient stock solutions was measured directly by FAAS.

Free ion concentrations of other trace metal nutrients in the media were computed from equilibrium calculations as described previously (Sunda and Huntsman, 1992,1995). The logs of the computed

Table 1
Relationships among total iron concentration, [Fe′], cellular iron concentration, carbon: volume ratio, Fe:C mole ratio, Chl:C mole ratio, mean volume per cell, specific growth rate (μ), iron uptake rate per liter of cell volume (v), maximum diffusion rate per liter of cell volume (ρ'), and ratio of iron uptake rate to the maximum diffusion rate (v/ρ')

Species (Exp.) Fe-tracer	Fetot (nM)	[Fe′] (pM)	Cell Fe (μmol l^{-1})	Cell C (mol l^{-1})	Fe:C (μmol mol^{-1})	Chl:C (mmol mol^{-1})	Cell vol (μm^3)	μ (d^{-1})	Uptake rate (v)	ρ'	v/ρ'
E. huxleyi											
(106) [a]	1.2	2.0					13.2	0.53			
^{55}Fe	2.3	3.9	66	(16) [b]	4.1	0.269	13.3	0.77	51	417	0.123
	4.3	7.1	79	(13)	6.0	0.427	13.7	0.92	72	750	0.096
	11.9	19.7	216	(13)	18.1	0.541	14.3	1.09	236	2020	0.117
	31.4	52	232	(12)	19.4	0.502	15.7	1.10	257	5010	0.051
	101	167	266	(12)	22.2	0.431	16.4	1.12	299	15700	0.019
(126)	1.2	3.0		17.7			17.9	0.70			
^{55}Fe	2.0	5.0	59	15.9	3.7	0.182	17.7	0.88	52	443	0.117
			50 [c]		**3.1** [c]				**44** [c]		**0.099** [c]
	3.9	9.7	138	12.5	11.0	0.303	20.2	0.99	136	793	0.172
			133		**10.7**				**132**		**0.166**
	9.7	24.2	165	12.4	13.3	0.346	20.2	1.10	181	1980	0.091
			160		**12.9**				**176**		**0.089**
	28.3	71	312	11.8	26.3	0.313	22.9	1.07	311	5330	0.062
			291		**24.6**				**331**		**0.058**
	101	253	341	10.3	33.2	0.387	21.8	1.04	354	19700	0.018
			464		**45.3**				**483**		**0.025**
	299	750	**295**	12.2	**24.2**	0.320	22.1	1.12	**330**	57700	**0.006**
(127a)	1.2	3.0		15.9		0.181	16.8	0.69			
^{55}Fe	2.0	5.1	66	16.3	4.1	0.210	16.9	0.95	62.9	470	0.134
	3.7	9.3	111	(13)	8.5	0.248	18.1	1.05	116	819	0.142
(127b) [d]	1.2	3.1		13.5		0.293	17.5	0.81			
(^{55}Fe)	2.0	5.1	73	16.1	4.6	0.180	18.6	0.89	65.3	440	0.148
	3.7	9.3	104	13.2	7.9	0.225	19.6	1.05	109	776	0.140
	7.7	19.3	134	13.7	9.8	0.245	21.5	1.18	158	1510	0.104
			113		**8.3**				**133**		**0.088**
	29	73	245	12.4	19.8	0.280	21.4	1.17	288	5780	0.050
	97	243	414	(12)	33.4	0.314	20.9	1.26	515	19400	0.026
			355		**28.6**				**447**		**0.023**
T. oceanica											
(98)	1.2	3.0		7.2			76	0.73			
^{55}Fe	4.2	10.6	42	8.6	4.9	0.193	75	1.10	46.4	361	0.128
			26		**3.0**				**28.8**		**0.080**
	11.2	28.2	65	9.1	7.1	0.186	88	1.36	88.2	866	0.102
			55		**6.0**				**74.2**		**0.086**
	30.9	78	110	9.8	11.3	0.196	96	1.55	171	2240	0.076
			89		**9.1**				**137**		**0.061**
	101	253	336	9.8	34.3	0.202	98	1.55	519	7200	0.072
			247		**25.2**				**382**		**0.053**
	303	760	**333**	9.8	**33.9**	0.206	103	1.58	**524**	20900	**0.025**
	1010		**458**	9.8	**46.7**	0.206	101	1.66	**762**		
(107) [a]	1.2	2.0					88	0.46			
^{55}Fe	2.4	3.9	19.1	7.5	2.5	0.239	81	0.67	12.9	126	0.102
	4.3	7.1	27.9	(7.8)	3.6	0.355	77	1.08	30.1	240	0.126
	11.7	19.3	46	8.1	5.7	0.354	80	1.27	58.4	629	0.093
	31.5	52	92	(9.0)	10.2	0.367	83	1.51	139	1660	0.084
	101	166	153	10.0	15.3	0.416	87	1.56	238	5120	0.046

Table 1 (continued)

Species (Exp.) Fe-tracer	Fetot (nM)	[Fe′] (pM)	Cell Fe (μmol l^{-1})	Cell C (mol l^{-1})	Fe:C (μmol mol^{-1})	Chl:C (mmol mol^{-1})	Cell vol (μm^3)	μ (d^{-1})	Uptake rate (v)	ρ'	v/ρ'
P. calceolata											
(116)	1.2	3.0						0.75			
^{55}Fe	2.2	5.5						0.91			
	4.3	10.7			13.3	0.286		0.95			
					8.4						
	12.1	30.3			21.1	0.331		0.96			
					8.5						
	31.6	80			22.3	0.279		1.03			
					8.1						
	100	252			**8.5**	0.322		1.05			
	232	580			**9.5**	0.356		1.03			
(139)	2.0	5.0			**4.3**	0.333		0.91			
^{59}Fe	4.2	10.5			**8.8**	0.310		0.95			
	11.2	28.0			**9.6**	0.347		0.98			
T. pseudonana											
(123)	9.5	23.9	194	15.6	12.5	0.170	22.3	0.50	98	1830	0.053
^{55}Fe			**200**		**12.9**				**101**		**0.055**
	29.4	74	354	14.3	24.7	0.234	22.9	1.04	369	5540	0.067
			327		**22.8**				**341**		**0.061**
	97.5	244	431	11.1	39.0	0.315	28.4	1.57	678	1590	0.040
			315		**28.5**				**495**		**0.031**
	290	730	**710**	10.5	**68.2**	0.314	31.8	1.80	**1290**	4390	**0.029**
	1023		**1600**	10.7	**149**	0.304	27.7	1.76	**2610**		
(135) [e]	4.3	10.3						0			
^{59}Fe	11.3	28.3	213	15.1	**14.1**	0.131	21.1	0.36	**77**	2250	**0.034**
	30.9	77	301	11.7	**25.6**	0.233	29.0	0.97	**293**	4970	**0.059**
	100	252	435	13.9	**31.2**	0.172	40.4	1.38	**601**	1300	**0.046**
	303	760	1000	14.4	**69.5**	0.189	43.4	1.68	**1680**	3730	**0.045**
	3010		4660	14.9	**313**	0.191	43.7	1.70	**7940**		
(138) ^{59}Fe	10000		**26500**	(15)	**1770**	0.258	46.1	1.37	**36400**		
T. weissflogii											
(113)	1.2	3.0						0			
^{55}Fe	2.2	5.5						0			
	4.3	10.8						0			
	11.0	27.6	131	(10)	13.1	0.127	750	0.32	42.0	203	0.173
			110		**11.0**				**35.2**		**0.085**
	21.9	55	138	(10)	13.8	0.246	720	0.51	70.2	412	0.170
			97		**9.7**				**49.4**		**0.120**
	108	271	215	(10)	21.5	0.352	850	0.86	184	1822	0.101
			262		**23.6**				**224**		**0.123**
	180	450	**287**	(10)	**30.4**	0.289	860	0.86	**247**	3010	**0.082**
			300	(10)	**30.0**				**258**		**0.086**
	301	750	**308**	(10)	**30.8**	0.327	900	0.89	**273**	4890	**0.056**
	1025		**1010**	(10)	**101**	0.313	890	0.89	900		
(138)	1000		**1230**	10.0	**123**	0.325	830	0.80	**980**		
^{59}Fe	3000		**2020**	9.9	**203**	0.338	850	0.80	1610		
	10000		**3350**	10.1	**333**	0.431	890	0.82	**2750**		

Table 1 (continued)

Species (Exp.) Fe-tracer	Fetot (nM)	[Fe′] (pM)	Cell Fe (μmol l^{-1})	Cell C (mol l^{-1})	Fe:C (μmol mol^{-1})	Chl:C (mmol mol^{-1})	Cell vol (μm^3)	μ (d^{-1})	Uptake rate (υ)	ρ'	υ/ρ'
P. minimum											
(137)	1.3	3.3						0.15			
^{59}Fe	4.3	10.7					750	0.24			
	9.3	23.2	**118**	11.0	**10.7**	0.135	970	0.28	**32.8**	144	**0.228**
	31.2	78	**203**	10.2	**20.0**	0.174	950	0.50	**103**	491	**0.210**
	101	252	**272**	10.9	**24.9**	0.160	1120	0.58	**159**	1420	**0.112**
	299	750	**364**	10.0	**36.5**	0.168	1140	0.57	**208**	4160	**0.050**
	1009		**630**	11.1	**56.6**	0.167	1220	0.56	**355**		
	2968		**780**	10.5	**74.5**	0.169	1220	0.61	**478**		

Uptake rate (υ) and maximum diffusion rate (ρ') are expressed in units of μmol Fe (liter cell volume)$^{-1}$ d^{-1}. The diffusion rate per unit of cell volume was obtained by dividing the rate per cell (ρ, see Eq. 2) by the mean volume per cell.

[a] Experiments 106 and 107 were run at light intensity reduced to 175 μmol quanta m^{-2} s^{-1}, 35% of the usual.

[b] Numbers in parentheses are estimated carbon values based on results from other experiments.

[c] Values for (or based on) intracellular iron are given in **bold**.

[d] For Exp. 127b, cells were grown with 32 μM ammonia rather than nitrate.

[e] For Exp. 135, log [Mn^{2+}] = −8.23 rather than normal value of −8.53.

free zinc, cobalt, manganese, copper and nickel ion concentrations were −10.99, −11.03, −8.53, −13.32 and −12.89, respectively.

Prior to experiments, cells were transferred from f/8 medium to an experimental medium with a sufficiently low iron concentration to limit growth rate. They were preacclimated for a period 6 to 12 days (depending on the growth rate) and were then inoculated into ^{55}Fe-or ^{59}Fe-labeled media at biomass levels of 0.1–0.2 μmol cell carbon per liter of medium. The algae were grown for 12–13 cell generations to the end of the exponential phase. For all species except *P. calceolata*, total cell concentrations and volumes were measured daily with a Coulter Counter (Model TAII) multichannel electronic particle counter and specific growth rates of cultures were computed from linear regressions of ln cell volume vs. time for the exponential phase of growth. *Pelagomonas calceolata* was too small to measure by Coulter Counter, and its growth rate was determined from daily ^{14}C-measurements of fixed carbon. In one experiment, the cultures were dual-labeled with ^{59}Fe and ^{14}C. However, in a prior experiment with ^{55}Fe, dual labeling was not possible and growth rates were measured in parallel cultures containing added ^{14}C (see below).

Intracellular and/or total cellular iron concentrations were measured with radiotracers (^{55}Fe or ^{59}Fe) in exponentially growing cultures, 9–10 cell divisions after inoculation. To measure total cellular iron, cells were filtered through 0.4, 1, or 3 μm pore Nuclepore filters (depending on cell size), and then rinsed with Gulf Stream water. To measure intracellular iron, cells retained on filters were rinsed for 2 min with a Ti-EDTA-citrate reducing solution to dissolve iron hydroxides and remove iron adsorbed to the cell surface (Hudson and Morel, 1989). The cellular ^{55}Fe retained on the filters was measured with a liquid scintillation counter (Beckman, LS 9000) and cellular ^{59}Fe was measured with an automatic gamma spectrometer (LKB Compugamma). The ^{55}Fe or ^{59}Fe activity in the cells was corrected for filter blanks of media without cells and was divided by the measured total activity of added radiolabel. These values were then multiplied by the total concentration of iron in the medium and divided by the measured total volume of cells to give cellular iron concentrations in units of mol Fe per liter of cell volume.

Cellular Fe:C ratios were also determined. In all cases cellular carbon was measured using standard ^{14}C liquid scintillation techniques (Welschmeyer and Lorenzen, 1984). For experiments with ^{59}Fe, ^{14}C was added directly to the experimental cultures containing radiolabeled iron. This dual labeling was possible since ^{14}C is a beta-emitting nuclide and does not

interfere with gamma counting of ^{59}Fe. To determine ^{14}C in the cells, however, the ^{14}C liquid scintillation counts had to be corrected for beta emission by ^{59}Fe. This was done by multiplying the measured ^{59}Fe gamma counts by an experimentally measured ratio of liquid scintillation (beta) to gamma counts for ^{59}Fe. As a check, the cells were recounted by liquid scintillation after 4–6 months, when > 85% of the short-lived (45-day half-life) ^{59}Fe had decayed away. During this time the activity of ^{14}C, whose half-life is 5000 yr, remained essentially unchanged.

Dual labeling was not feasible with ^{55}Fe, the radiolabel used in most experiments. In experiments with this radionuclide, cellular Fe:C ratios were determined by dividing the Fe to cell volume values by carbon to cell volume ratios measured in separate parallel cultures without ^{55}Fe. These ratios were 12–16, 7–10, 11–16, ~ 9, and 13–15 mol C l^{-1} for *E. huxleyi*, *T. oceanica*, *T. pseudonana*, *T. weissflogii*, and *P. minimum*, respectively (Table 1). In addition to the above measurements, mean volume per cell and chlorophyll *a* concentrations were also determined. Mean volume per cell was measured by Coulter Counter.

Since a Coulter Counter could not be used to quantify cell volumes of *P. calceolata*, an alternative method was used to measure cellular Fe:C ratios in an initial ^{55}Fe experiment with this isolate. In this experiment, the cellular iron concentrations were normalized to chlorophyll *a* and these values were then divided by chlorophyll *a*:carbon ratios determined in parallel cultures containing ^{14}C-bicarbonate and no ^{55}Fe. In a subsequent experiment with this isolate, dual labeling of the cultures with ^{59}Fe and ^{14}C was utilized to quantify cellular Fe:C ratios.

3. Results

Cellular growth rate, chlorophyll *a*, and mean cell size all decreased with decreasing iron concentrations (Table 1; Fig. 1). In contrast, there was no consistent trend among species in effects on cell carbon to volume ratios. *Thalassiosira oceanica* showed a 25% decrease in cell C:volume ratios with decreasing [Fe′] while *E. huxleyi* exhibited an ~ 30% increase (Table 1). *Thalassiosira pseudonana* and *P. minimum* showed no consistent trend.

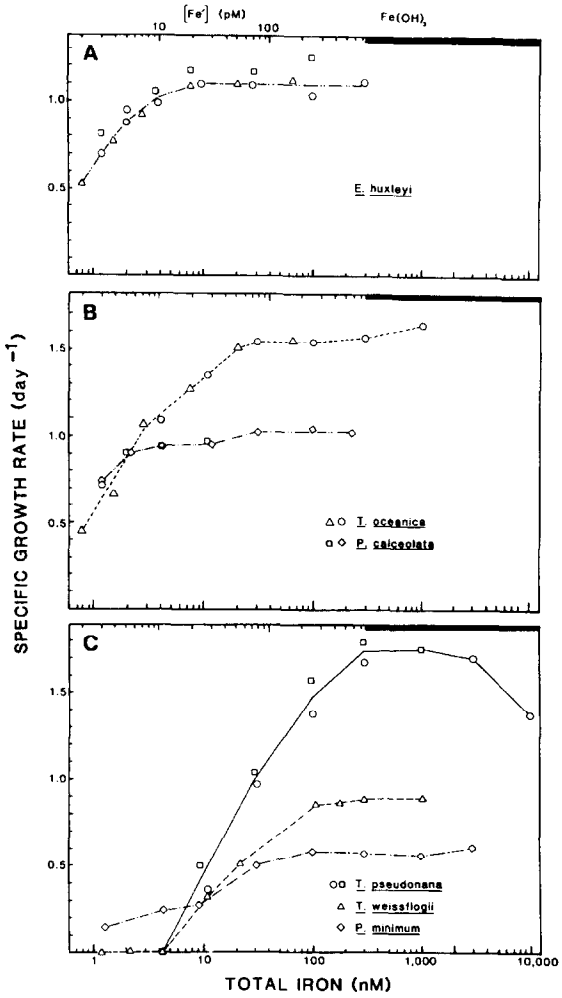

Fig. 1. Relationships between specific growth rate and total iron concentration or mean [Fe′] in the medium. (A) Results for *E. huxleyi* (Exps. 106, △; 126 and 127a, ○; and 127b, □). For Exp. 127b ammonium was substituted for nitrate as the nitrogen source. Also in Exp. 106, the light intensity was reduced to 35%. (B) Results for *P. calceolata* (Exps. 116, ◇; and 139, □) and for *T. oceanica* (Exp. 98, ○, at full light; and 106, △, at 35% light). (C) Results for *T. pseudonana* (Exps. 123, □; and 135 and 138, ○), *T. weissflogii* (Exp. 113, △), and *P. minimum* (◇). Growth rate of reduced light experiments (106 in A and 107 in B) are plotted only as functions of [Fe′]; because of photodissociation, total iron concentrations in these experiments are 1.5 times higher than values on the bottom axis. Solid bar on the right portion of the [Fe′] axis indicates the region where iron hydroxides are precipitating, and therefore [Fe′] cannot be estimated.

Differences occurred among species in their chlorophyll response to low iron stress. *Thalassiosira weissflogii* exhibited a 60% decrease in cellular Chl *a*:carbon ratios with decreasing [Fe′] while other species showed 10–50% declines (Table 1). All species that could be measured (all except *P. calceolata*) showed a 18–50% decrease in mean volume per cell in response to reduced iron concentrations (Table 1). Decreased cell size was also associated with reduced light intensity, an effect that was most evident for *E. huxleyi* (Table 1).

Light was decreased from 500 to 175 μmol quanta m^{-2} s^{-1} in one experiment each with *T. oceanica* and *E. huxleyi*. Reduction in light intensity had no effect on maximum growth rate, indicating saturating light conditions for photosynthesis. Reduced light, however, increased iron limitation of growth rate, an effect that was entirely accounted for by the 35% reduction in mean [Fe′] values at the lower light intensity (Table 1; Fig. 1A,B). The decrease in [Fe′] resulted from a decrease photodissociation of Fe(III)-EDTA chelates, as described by Anderson and Morel (1982). Although it had no direct effect on growth rate, reduced light was associated with up to two-fold increases in Chl:C ratios due to photoadaptation (Table 1, Exps. 106 and 107).

As in previous studies, there was a clear difference between coastal and oceanic isolates in their growth response to iron limitation (Fig. 1). The three oceanic isolates were able to grow at a reduced rate of about 0.7 d^{-1}, at [Fe′] of 3 picomolar, while the coastal diatoms (*T. pseudonana* and *T. weissflogii*) needed [Fe′] of 40 and 120 pM, respectively, to achieve the same iron-limited growth rate. The coastal diatoms were unable to grow at all at [Fe′] of 10 pM. *Prorocentrum minimum* exhibited an unusual bimodal iron limitation curve in which there was a rapid (52%) reduction in growth rate as [Fe′] was reduced from 250 to 25 pM, but little further reduction in growth at lower [Fe′]. At the lowest experimental [Fe′] of 3 pM, *P. minimum* still had a finite growth rate of 0.15 d^{-1}.

Both intracellular and total cellular iron concentrations were measured for most species (but not necessarily in all experiments; Table 1). Intracellular iron was 75 ± 10% of total cell iron in *T. oceanica* and 90 ± 6% in *E. huxleyi*, similar to previously measured values for phytoplankton (Hudson and Morel, 1990; Sunda et al., 1991). In *P. calceolata*, however, it was 63% of total cellular iron at [Fe′] of 11 pM and decreased to 35% at [Fe′] of 30 and 80 pM. These values are probably erroneously low because in 3 of 4 treatments in a subsequent experiment, the Ti-EDTA-citrate wash used to measure intracellular iron caused 47%–52% decreases in cell carbon values, indicating cell leakage or lysis. Although we found no evidence for such artifacts in other species, the results with *P. calceolata* indicate that caution should be used in applying the Ti-EDTA-citrate wash method to field plankton samples of unknown composition.

Because of precipitation of iron hydroxide, total cellular iron (including that adsorbed to the cell surface) could not be measured at [Fe′] values ≤ 0.75 nM (300 nM total iron at the high light intensity) (Fig. 2). This precipitation also prevented computation of [Fe′] at total iron concentrations > 300 nM.

Curves for cellular Fe:C vs. Fe concentration in the medium had positive slopes, but exhibited differ-

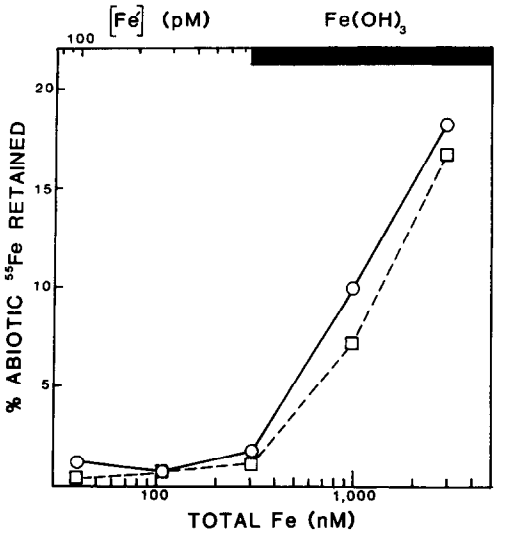

Fig. 2. Percentage of total iron present as abiotic iron retained on 3 μm filters vs. total iron concentration and computed mean [Fe′]. Data are for cultures of *T. pseudonana* incubated for 3–5 days (○) and for culture media without cells incubated for 5 days (□). Particulate abiotic iron in the cultures equals the particulate iron that is dissolved by exposure to a Ti-EDTA-citrate reducing solution. Thus, it also includes iron adsorbed to the cell surface. The large increase in abiotic particulate iron at [Fe′] > 750 pM results from precipitation of iron hydroxides.

ent shapes that were largely habitat related (Fig. 3). Curves for the three oceanic species showed highest slopes at low concentrations and decreasing slopes at higher levels. For *E. huxleyi*, intracellular Fe:C reached a plateau of 25–30 μmol mol^{-1} at [Fe′] > 80 pM, while for *P. calceolata*, total cellular Fe:C reached a similar plateau of ~ 23 μmol mol^{-1} at [Fe′] > 30 pM. By contrast, the coastal diatoms never did show a plateau, even when total iron in the medium was increased to 10 μM, well into the region where iron hydroxides were precipitating. Intracellular Fe:C reached a value of 1700 μmol mol^{-1} in *T. pseudonana*, 30 times higher than needed to support maximum growth rate, and 50–70 times higher than the plateau values for *E. huxleyi* and *P. calceolata*.

Net steady-state iron uptake rates, V_{ss} (in units of μmol Fe per liter of cell volume per day [Fig. 4Fig. 5] or per mole of cell carbon per day [Fig. 6]), were computed by multiplying cellular iron concentrations by specific growth rate:

$$V_{ss} = [\text{cell iron}]\,\mu \quad (1)$$

The curves for iron uptake rate vs. [Fe′] or total iron showed regions at lowest iron concentrations where the iron accumulation rates were proportional or nearly proportional to the external concentration, followed by decreasing slopes at higher concentrations (Figs. 4, 5). The regions of minimal slope are apparently due to feedback regulation of cellular iron transport as based on previous studies of iron uptake by *T. weissflogii* (Harrison and Morel, 1986) and uptake of other trace metal nutrients, such as manganese and zinc, by many of the same species examined here (Sunda and Huntsman, 1985,1986, 1992). For *T. pseudonana*, there was a second acceleration in iron uptake rates at total iron concentrations above 1000 nM, coinciding with the region of iron hydrox-

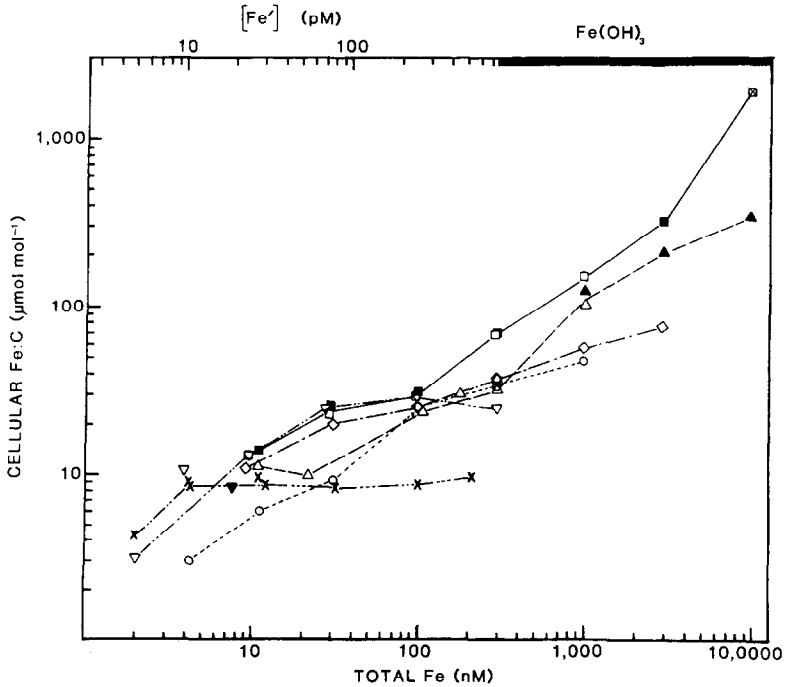

Fig. 3. Relationship between intracellular Fe:C ratio and total iron concentration (or [Fe′]) for *E. huxleyi* (Exp. 126, ▽; and 127, ▼), *T. oceanica* (Exp. 98, ○), *P. calceolata* (Exps. 116 and 139, ×), *T. pseudonana* (Exp. 123, □; 135, ■; and 138, ⊠), *T. weissflogii* (Exp. 113, △; and 138, ▲), and *P. minimum* (◇). All data shown are for normal light conditions (500 μmol quanta m^{-2} s^{-1}).

ide precipitation (Fig. 5). No other species showed any acceleration of iron uptake within this region.

The ability of cells to grow at low iron concentrations is determined by both their uptake rate per unit of biomass (Fig. 6) and growth rate per mole of cellular iron [i.e. mol C (mol Fe)$^{-1}$ d^{-1}, the iron use efficiency]. It is clear from our results that variations in biomass specific uptake rates are at least partly responsible for the ability of the oceanic species to outgrow coastal species at low iron concentrations (Fig. 6). At low [Fe′] all three oceanic species had higher biomass specific uptake rates than the coastal species. At [Fe′] of 25 pM (the lowest value for which direct comparisons among all species could be made), biomass specific rates varied from 20 μmol (mol C)$^{-1}$ d^{-1} for *P. calceolata*, the small oceanic flagellate, to 3–4 μmol mol^{-1} d^{-1} for *T. weissflogii* and *P. minimum*, the two large coastal species. Uptake rates per unit of cell volume showed a similar pattern of variation (Fig. 5), except that on a per volume basis, the coastal diatom, *T. pseudonana*, had higher uptake rates at equivalent iron concentrations than its larger oceanic congener, *T. oceanica*, due to its higher carbon to cell volume ratio (Table 1).

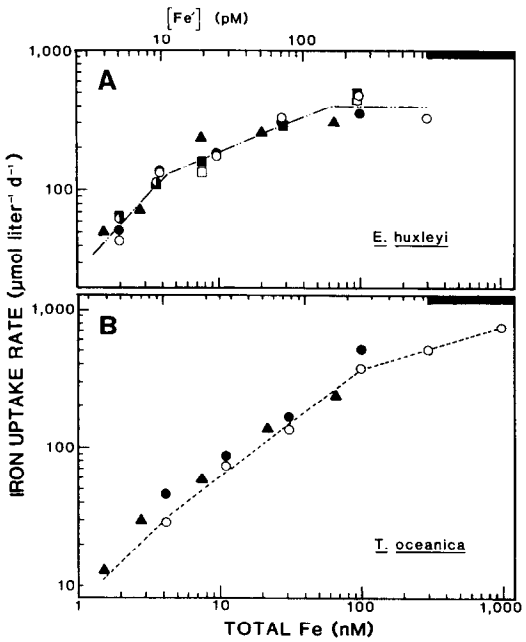

Fig. 4. Relationships between the iron uptake rate per liter of cell volume and total iron concentration or [Fe′]. (A) Data for *E. huxleyi*, Exp. 126 (○●) and 127a (◑) (nitrate, full light intensity); Exp. 106 (▲) (nitrate, 35% light); and 127b (□ ■) (ammonium, full light). (B) Data for *T. oceanica*, Exp. 98 (○●) at full light and 107 (▲) at light intensity reduced to 35%. As in Fig. 1, rates for reduced light experiments (106 in A and 107 in B) are plotted only as functions of [Fe′] and total iron concentrations in these experiments are 1.5 times higher than values shown on the bottom axis. Solid bar on the right portion of the [Fe′] axis indicates the region where iron hydroxides are precipitating. Open and closed symbols indicate uptake rates of intracellular and total cellular iron, respectively. Curves drawn are for intracellular iron uptake.

When iron uptake rates were normalized on a per cell surface area basis, the differences among species disappeared for four of the five species for which such rates could be estimated (Fig. 7). On a per surface area basis, iron uptake rates at low [Fe′] were nearly identical for *T. oceanica*, *T. pseudonana*, *T. weissflogii*, and *P. minimum*. The surface area normalized rates of *E. huxleyi* at lowest [Fe′], however, were 2–3 times those for *T. oceanica*. Thus, most of the differences among species in their ability to take up iron was due to differences in cell size and resulting effects on surface to biomass ratios.

In addition to more favorable transport rates (largely related to smaller cell size), much of the capability of oceanic species to grow better than coastal species at low iron concentrations was related to a substantial reduction in their growth requirements for cellular iron (i.e. to a higher iron use efficiency) (Fig. 8). To achieve a specific growth rate of 0.8 day^{-1}, the two coastal diatoms required about 20 μmol of intracellular Fe per mole of carbon whereas the oceanic diatom and coccolithophore needed only 2.3 and 3 μmol mol^{-1}, respectively.

4. Discussion

4.1. Physical / chemical limits on iron uptake

Our results indicate that the iron uptake rates per unit of cell surface are similar for four of five species and are not that much higher for *E. huxleyi*. They also appear to be similar for *P. calceolata*, the oceanic flagellate that was too small for direct measurements of cell volume. For this species we can estimate uptake per unit of cell surface area from the measured values of iron uptake per unit of cell

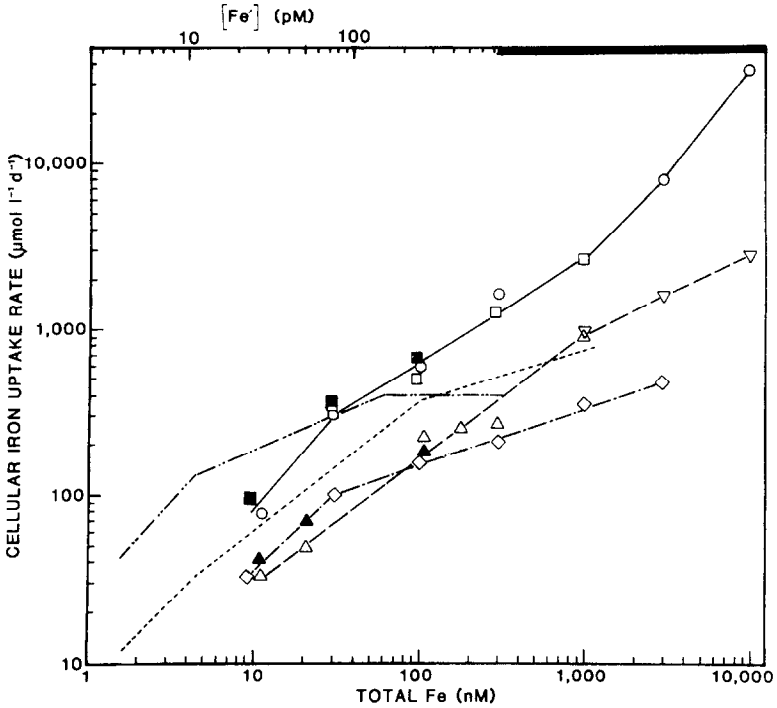

Fig. 5. Relationships between the iron uptake rate per liter of cell volume and total iron concentration or [Fe′] for *T. pseudonana* (Exp. 123, □ ■; and 135 and 138, ○), *T. weissflogii* (△ ▲ ▽), and *P. minimum* (◇). Open and closed symbols indicate uptake rates of intracellular and total cellular iron, respectively, and curves drawn are fit to the intracellular data. For comparison, intracellular uptake curves for *E. huxleyi* (– · · –) and *T. oceanica* (- - -) from Fig. 4 are shown.

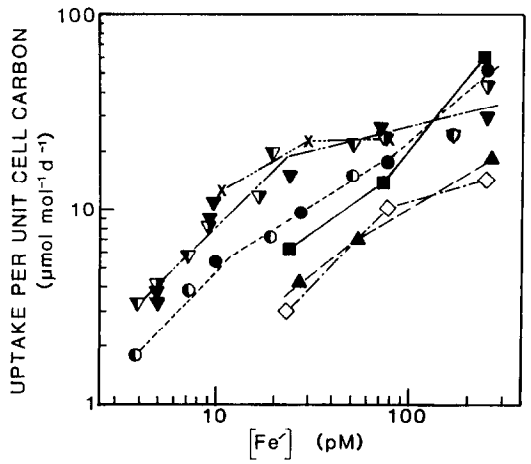

Fig. 6. Relationships between cellular iron uptake rate per unit of cell carbon and computed mean [Fe′] for *P. calceolata* (×), *E.* huxleyi (Exps. 106, ▼; 126 and 127a, ▾; and 127b, ⧩), *T. oceanica* (Exps. 98, ●; and 107, ◑), *T. pseudonana* (Exp. 123, ■), *T. weissflogii* (▲), and *P. minimum* (◇). All data are for total cellular iron uptake except that for *P. minimum*, which is for intracellular iron uptake.

carbon (Fig. 6) and an assumed carbon to volume ratio of 12 mol l^{-1} (a typical value for smaller cells; Table 1) and a mean cell radius of 1.0 μm, based on microscopic examination. At [Fe′] = 11 pM, the carbon normalized uptake rate was 12.7 μmol mol^{-1} d^{-1}, and based on the above cell radius and C:volume estimate, this value converts to an uptake rate per unit surface area of 0.51 μmol m^{-2} d^{-1}, close to the value for *T. oceanica* (0.40 μmol m^{-2} d^{-1}) at the same [Fe′].

The similarity in surface area normalized uptake rates is curious since we would have expected oceanic species to have evolved much more effective transport systems to adapt to the much lower iron concentrations in their environment. Hudson and Morel (1990) examined iron uptake in *T. weissflogii* (Actin), one of the coastal clones studied here, and found that uptake occurred via the exchange of iron between kinetically labile dissolved hydrolysis species (Fe′) and membrane transport ligands. Furthermore, they observed that iron uptake rates were near their maxi-

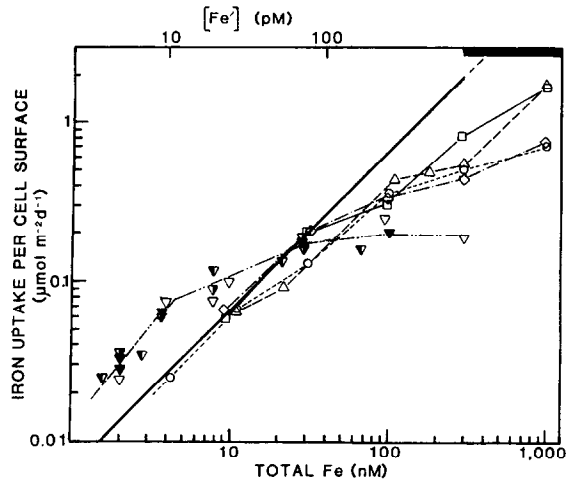

Fig. 7. Relationships between uptake rate per unit of surface area and total iron concentration (or mean [Fe′]) for *E. huxleyi* (Exps. 106, ▼; 126 and 127a, ▽ ▼; and 127b, ⧩), *T. oceanica* (Exp. 98, ○), *T. pseudonana* (Exp. 123, □), *T. weissflogii* (△), and *P. minimum* (◇). Data for all species except *E. huxleyi* are for uptake of intracellular iron. For *E. huxleyi* intracellular iron values are given as open symbols and total cellular iron values are given as closed or half filled symbols. Uptake rates per unit of cell surface area were computed by multiplying rates per unit volume by an estimated surface to volume ratio, computed from the mean volume per cell by assuming a spherical geometry. As before, rates for reduced light experiments (106 and 107) are plotted only as functions of [Fe′] and total iron concentrations in these experiments are 1.5 times higher than values shown. The solid diagonal line of unity slope gives a computed theoretical uptake rate based on the kinetics of iron exchange between Fe′ and a membrane transport ligand (Rate = k_f [Fe′] M_T, after Hudson and Morel, 1993). In these calculations, the ligand exchange constant for Fe′ in seawater, k_f, was assigned a value of 2×10^6 M^{-1} s^{-1}, the same as the rate constant for reaction of Fe′ with the siderophore deferriferrioxamine B (Hudson and Morel, 1990). The moles of transport site per meter of surface area, M_T, was computed by assuming that the transporter is a permease with the same cross sectional area (1.66×10^{-17} m^2) as a calcium ATPase (Hudson and Morel, 1993) and that these sites occupy 15% of the membrane area.

mum physical limits based on diffusion of Fe′ to the cell surface and ligand exchange kinetics for reaction of Fe′ with membrane uptake sites. They concluded, therefore, that for a species to grow at the extremely low dissolved iron concentrations that exist in the open ocean, it either would have to be much smaller (generating a more favorable surface to volume ratio and smaller surface diffusion layer) or would have to have a much lower cellular iron requirement for growth.

Our results generally support their conclusion. Thus, the reason why the iron transport rates of the oceanic species are not much faster than those of coastal species is because the coastal species are already transporting iron at rates approaching the

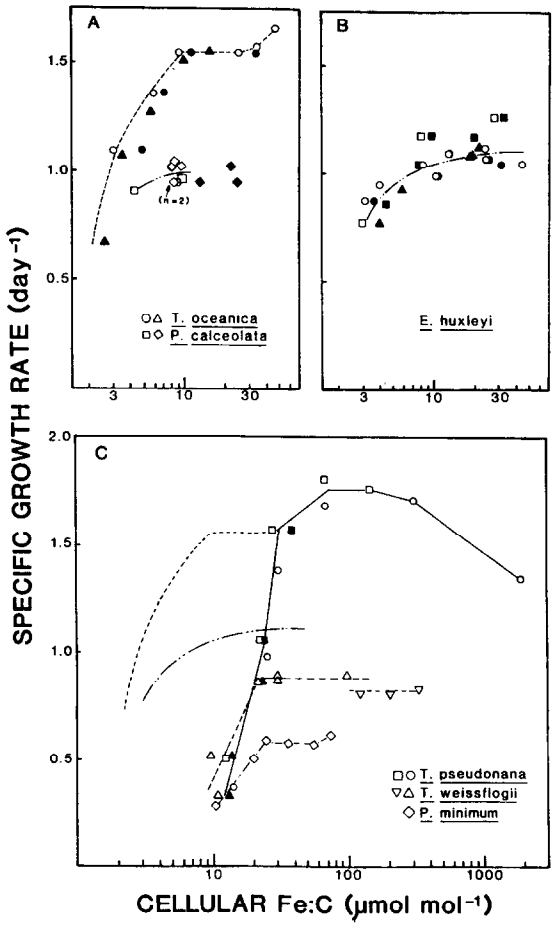

Fig. 8. Relationships between specific growth rate and cellular Fe:C ratios. (A) Data for *P. calceolata* (Exps. 116, ◇◆ and 139, □) and *T. oceanica* (Exp. 98, full light, ○●; and 107, 35% light, ▲). (B) Data for *E. huxleyi* (Exps. 126 and 127a, nitrate, full light, ○●; Exp. 106, nitrate, 35% light, ▲; and 127b, ammonium, full light, □ ■). (C) Data for *T. pseudonana* (Exp. 123, □ ■; and 135 and 138, ○), *T. weissflogii* (△ ▲ ▽), and *P. minimum* (◇). As before open and closed symbols indicate intracellular and total cellular Fe:C values, respectively. Curves drawn are for intracellular Fe:C. Curves for *T. oceanica* in A (- - -) and *E. huxleyi* in B (– · ·) are also shown in C for comparison.

physical limits imposed by ligand-exchange kinetics and diffusion. Our results suggest that limitation by ligand exchange kinetics may be more important than diffusion limitation, especially for smaller cells. Ligand-exchange limitation will be related to maximum rate at which iron can react with a single transport ligand times the maximum number of these ligands that can fit onto the cell's outer membrane, given the spatial needs for other essential membrane functions (Hudson and Morel, 1990). Ultimately such limitation will be controlled by the cell's surface area, and transport rates of different sized cells should be similar when normalized to this parameter, which is what we observed. We note that our surface area normalized uptake rates agree well with theoretically modeled rates based ligand-exchange kinetics for Fe′ in seawater and reasonable estimates for the diameter of iron transport sites (2.3 nm, the same as a calcium ATPase membrane calcium pump) and the percentage of the surface membrane occupied by these sites (15%) (Fig. 7).

For ligand-exchange limitation of transport, uptake per unit of biovolume should be inversely related to the cell diameter, but diffusion limitation of transport has a higher order dependence on cell size. Hydrodynamic models indicate that the maximum diffusion rate, ρ, of soluble labile iron species to a single cell is proportional to the mean cell radius, r:

$$\rho = 4\pi rD[\mathrm{Fe}'] \qquad (2)$$

where D (9×10^{-6} cm^2 s^{-1} at 20°C) is the diffusion coefficient for labile inorganic iron species (Paschiak and Gavis, 1974; Hudson and Morel, 1990). Since cell volume is proportional to the cell radius cubed, the above equation indicates that under diffusion limitation, uptake rate per volume of cells will vary as the inverse square of the cell diameter. Thus, diffusion limitation becomes disproportionately more important as the cell diameter increases (Hudson and Morel, 1993). Computations indicate that at low iron concentrations, the observed intracellular uptake rates range from 4–6% of the maximum diffusion rate for *T. pseudonana*, the small coastal diatom, to 17–23% of maximum rates for the two large coastal species (Table 1). Thus, diffusion limitation of transport begins to become important for the larger, 11–12 μm diameter cells, but is a lesser factor for smaller cells.

Physical/chemical limitation of uptake rates, similar to that observed for iron, also has been observed for zinc uptake by four of the species examined in this study: *E. huxleyi*, *T. oceanica*, *T. pseudonana*, and *T. weissflogii* (Sunda and Huntsman, 1992). For zinc, the observed uptake rates were 30–100% of the computed maximum diffusion rates, indicating that diffusion limitation is more important for zinc than it is for iron. For zinc, diffusion kinetics rather than ligand exchange kinetics appears to be the most important factor limiting cellular uptake rates, consistent with the ~20-fold higher ligand exchange rates for inorganic zinc species in seawater compared to those for Fe′ (Hudson and Morel, 1993).

The similarity in surface area normalized uptake rates among the species suggests that they all utilize the same uptake mechanism, namely the reaction of Fe′ species with membrane-bound transport ligands, the mechanism identified for *T. weissflogii* (Hudson and Morel, 1990). There is increasing evidence, however, for the importance of an additional uptake mechanism in marine microorganisms, involving the extracellular release of soluble siderophores and subsequent membrane transport of iron-siderophore chelates (Trick, 1989). *Prorocentrum minimum*, the dinoflagellate we studied here, is known to produce a hydroxymate siderophore under iron limiting conditions (Trick et al., 1983), and the release of such a ligand could explain the bimodal shape of its growth rate vs. iron concentration curve, and explain why this species was still able to grow at the lowest iron concentration (Fig. 1C). Also, the two-to three-fold higher surface area normalized uptake rates observed for *E. huxleyi* (Fig. 7) could be related to the use of soluble siderophores.

Since coastal species appear to be transporting iron near maximum rates permitted by physics and chemistry, oceanic species have had essentially three choices in order to adapt to the extremely low iron concentrations in the open sea: (1) they could become smaller or take on irregular shapes which increases their surface to biomass ratio, (2) they could grow slower which decreases the rate at which cell iron is diluted by growth (see Eq. 1) and decreases the metabolic demand for iron containing enzymes (cytochromes and FeS proteins), or (3) they could decrease their growth requirement for cellular iron. All three of these appear to have occurred.

Oceanic phytoplankton generally have lower growth rates than coastal plankton, and oceanic environments that are thought to be the most iron limited, such as the Southern Ocean and the subarctic and equatorial Pacific, are dominated by extremely small cells (Miller et al., 1991).

The 20–50% decrease in volume per cell observed for both coastal and oceanic species, itself represents an adaptation to low iron availability since it increases surface to volume ratios by 8–26%. Ultimately, however, the biomass normalized uptake rate (rather than the biovolume normalized rate) is most important; and, therefore, it is also advantageous for a cell to decrease its biomass to volume ratio, for example, by increasing the size of its vacuole. Under iron limitation of growth, *T. oceanica* maintained a C:cell volume ratio that was only about half that of *T. pseudonana* (Table 1), thus, allowing it to maintain a higher iron uptake rate per unit of cell carbon despite its larger size. This species decreased its cell C:volume ratio by 27% and its mean volume per cell by 26% in response to iron limitation, and the effect of both factors yielded a 50% increase in cell surface area to carbon ratio with decreasing [Fe′] (Table 1, Exp. 98).

4.2. Luxury iron uptake and storage

The ability to take up and store iron in excess of levels needed to meet immediate metabolic needs represents an additional important aspect of a species' overall iron acquisition strategy. The ability for luxury uptake would be most advantageous for species living in coastal waters where iron concentrations are high, but spatially and temporally variable. It would also be of greatest benefit to species, such as diatoms, that bloom episodically under conditions of high major nutrient availability and favorable light.

The patterns of luxury iron uptake that we observed among the species generally fit these predictions. The largest luxury uptake occurs in the three diatoms, which bloom episodically, and is especially high in the two coastal species, *T. weissflogii* and *T. pseudonana*. For these two species, cellular Fe:C reached values that were 20–30 times higher than those needed for maximum growth. By contrast, maximum or "plateau" iron concentrations in the oceanic coccolithopore and coastal dinoflagellate were only two to three times higher than maximum needed amounts.

The high iron uptake and storage capacity in the coastal diatoms allows these species to accumulate excess iron during periods of high availability and/or low growth rate (low dilution rate, see Eq. 1), which then can be drawn upon later in periods of high growth rate during blooms. Their high capability to store iron may be an important factor in allowing diatoms to outcompete other species during episodic blooms. The ability to take up and store large quantities of iron, however, is not without hazard since high iron levels can be quite toxic. In *T. pseudonana* sufficient iron was taken up at the highest iron concentration for the metal to inhibit growth rate (Fig. 8).

An intriguing aspect of iron uptake in *T. pseudonana* is the acceleration in uptake rates at the highest iron concentrations (1–10 μM), within the region where iron hydroxides are precipitating (Fig. 5). This behavior suggests that uptake in this species may not be simply related to soluble [Fe′] as reported for *T. weissflogii* (Hudson and Morel, 1990). Rather, at high iron concentrations, *T. pseudonana* may possess mechanisms, such as thermal or photochemical reduction, to directly access iron present in hydroxide particles adsorbed to the cell surface.

4.3. Variations in metabolic requirement

One of the most important evolutionary responses to low iron concentrations in the open ocean, is a substantial reduction in the cellular growth requirement for iron. The growth requirements for the three coastal species are similar to one another, and are surprisingly close to theoretical iron use efficiency values calculated from the amounts of metabolic iron needed to support photosynthesis, respiration and nitrate reduction (Fig. 9). By contrast, the cellular iron requirements for growth of oceanic species, *E. huxleyi* and *T. oceanica*, are six to eight times lower. Similar findings of low cellular iron requirements of oceanic eucaryotic species have been reported by Brand (1991), based on iron yield experiments with 10 oceanic and 5 coastal species from a variety of eucaryotic algal groups. Curiously, Brand found an unusually high iron requirement in species of *Synechococcus*, and found less distinct coastal/oceanic differences for this cyanobacterial genus.

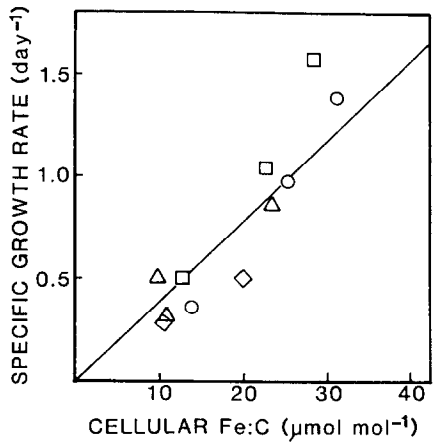

Fig. 9. Relationship between specific growth rate of iron-limited cells and intracellular iron concentration for coastal species: *T. pseudonana* (Exp. 123, □; and 135, ○), *T. weissflogii* (△), and *P. minimum* (◇). Data agree well with values estimated from theoretical iron use efficiencies (solid line) computed by Raven (1988). Raven (1988) computed that cells would need an Fe:C ratio of 38 μmol mol^{-1} to meet metabolic demands for photosynthesis, respiration, and nitrate assimilation in order to grow at a specific rate of 2.7 d^{-1} under saturating continuous light. For a 14:10 daily light:dark cycle, as used in our experiments, we have assumed that the daily specific rate would be equal to the continuous light value (2.7 d^{-1}) times the fraction of the day that the cells received light (14/24 = 0.58). For the theoretical relationship in the figure, we have further assumed that the specific growth rate is simply proportional to the cellular Fe:C ratio. Note that these calculations implicitly ignore any iron cost for dark and light maintenance respiration and ignore metabolic iron costs for other processes such as removal of hydrogen peroxide.

The mechanisms by which oceanic eucaryotic phytoplankton have been able to reduce their growth requirements for cellular iron are unknown. Possibilities include more efficient use of intracellular pools, minimization (or avoidance) of metabolic pathways that require large amounts of iron, and replacement of iron containing proteins with those without a metal catalyst or with those possessing other, more abundant, transition metal catalysts. For example, many algae can replace ferredoxin, which contains two iron atoms per molecule, with flavodoxin, a larger functionally equivalent non-metalloprotein (Entsch et al., 1983; Raven, 1988; La Roche et al., 1993). Also, in photosynthetic electron transport, iron-containing cytochrome c-553 can be replaced by plastocyanin, which contains copper (Wood, 1978). Other possibilities include replacing Fe-superoxide dismutase with Mn-SOD and replacing catalase and Fe-peroxidases with glutathione peroxidase, which contains selenium rather than iron.

The major requirement for iron is in the photosynthetic electron transport chain where there are an estimated 26 iron atoms in cytochromes and Fe/S proteins per photosynthetic unit (Raven, 1988). That number is reduced to 23 in cases where flavodoxin and plastocyanin replace their iron containing analogs. If we assume that there are roughly 600 chlorophyll *a* molecules per photosynthetic unit (based on the value for *Skeletonema costatum* at saturating light; Falkowski et al., 1981), then we compute an Fe:Chl *a* ratio in the chloroplast of 38 mmol mol^{-1}. This number falls in the middle of the range of values we measured under iron limitation of growth rate (Fig. 10). The coastal species had Fe:Chl

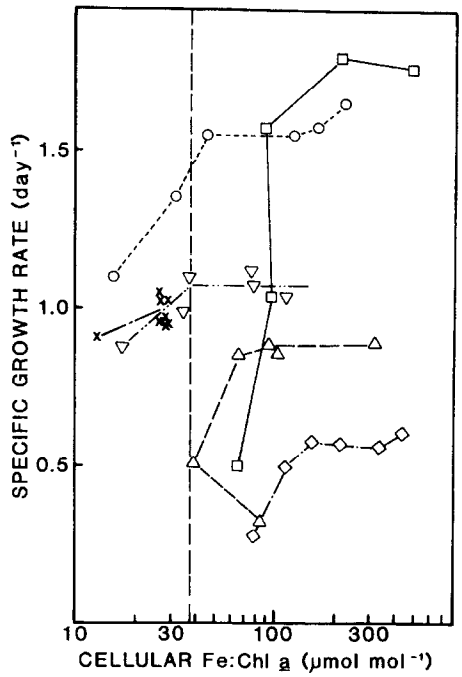

Fig. 10. Relationship between specific growth rate and intracellular Fe:Chl *a* for *P. calceolata* (Exps. 116 and 139, ×), *E. huxleyi* (Exp. 126, ▽); *T. oceanica* (Exp. 98, ○), *T. pseudonana* (Exp. 123, □), *T. weissflogii* (Exp. 113, △), and *P. minimum* (◇). Data given are only for full light conditions (500 μmol quanta m^{-2} s^{-1}) and nitrate as a nitrogen source. Vertical dashed line represents a computed Fe:Chl *a* ratio (in the chloroplast) of 38 mmol mol^{-1} based on literature values of 23 iron atoms and 600 Chl *a* molecules per photosynthetic unit.

a ratios of 40–100 mmol mol^{-1} under iron limitation, while oceanic species had values of 11–30 mmol mol^{-1}, below the stoichiometric estimate for photosynthetic units.

Reduction of nitrate to ammonia represents the next highest metabolic demand for iron (Raven, 1988). Based on biochemical calculations, cells growing on nitrate should require 40–50% more iron than cells supplied with ammonia (Raven, 1988; Morel et al., 1991). In contrast to this prediction, cells of *E. huxleyi* grown on nitrate did not show a higher iron requirement than cells grown on ammonia (Table 1; Fig. 8b). Apparently, the additional iron needed for nitrate reduction in this species is small and is within our experimental error.

4.4. Relationship of culture data to iron distributions and speciation in seawater

Recent radiotracer studies indicate that iron is rapidly cycled within the planktonic community and is subject to the same uptake and regeneration processes as occur for major nutrients (Hutchins et al., 1993). Uptake and regeneration of nutrients causes their depletion in surface waters and enrichment at depth, resulting in pronounced increases in concentrations with depth within the upper 600–1000 m (the nutricline). As a result of uptake and regeneration, the concentrations of phosphate and nitrate with depth are linearly correlated with one another and the slopes of N vs. P regressions ($\sim$ 16:1) equal the ratio of N to P found in phytoplankton (Redfield et al., 1963). These ideas were originally developed for major nutrients (N, P, and C) by Alfred Redfield during the early 1930s (Redfield, 1934), but have recently also been applied to micronutrients such as zinc and copper (Sunda and Huntsman, 1992, 1995).

Recent measurements indicate severe depletion of iron in the oceanic euphotic zone and increased concentrations with depth, similar to the pattern observed for N and P. The concentrations of dissolved or total iron are generally closely correlated with those of nitrate or phosphate, supporting the idea that iron distributions, like those of other nutrients, are controlled by biological uptake and regeneration (Table 2). If true, then the slopes of regressions of iron vs. phosphate concentrations with depth provide an indicator of Fe:P ratios in plankton, and by inference, Fe:C ratios. Regressions of total or dissolved iron concentrations vs. phosphate within oceanic nutriclines yield Fe:P slopes of 240–300 μmol mol^{-1} in the North Pacific and 420 μmol mol^{-1} in the North Atlantic (Table 2). These values convert to Fe:C ratios of 2.2–2.6 and 4.0 μmol mol^{-1}, respectively, assuming a "Redfield" carbon:phosphate ratio in plankton of 106:1. Such Fe:C ratios would be

Table 2
Slopes of iron vs. phosphate regressions for oceanic nutriclines and resulting estimates of Fe:C in phytoplankton

Location	Depth range (m)	n	Slope (μmol mol^{-1})	r^2	Fe:C [a] (μmol mol^{-1})	Reference [b]
N. Pacific						
33.3°N 139.1°W	50–790	8	249 [c]	0.950	2.3	1
		7 [d]	264 [c]	0.994	2.5	
39.6°N 140.8°W	50–900	9	242	0.972	2.3	2
45.0°N 142.9°W	50–800	7	236	0.983	2.2	2
50.0°N 145.0°W	25–780	12	271	0.940	2.6	2
N. Atlantic						
47°N 23°W	20–900	9	424	0.945	4.0	3

[a] Values computed by dividing Fe:P slope by the "Redfield" C:P ratio of 106:1.
[b] 1 = Martin and Gordon, 1988; 2 = Martin et al., 1989; 3 = Martin et al., 1993.
[c] Regression of total (dissolved plus particulate) iron concentration vs. phosphate. All other regressions are for dissolved iron vs phosphate.
[d] One outlying data point omitted. Note much higher r^2.

insufficient to meet the metabolic requirements of our coastal species, but would be adequate to support the growth of oceanic species at iron-limited rates. For example, at the mean Fe:C ratio of 2.4 μmol mol^{-1}, estimated from iron and phosphate distributions in the North Pacific (Table 2), *T. oceanica* would be able to grow at an iron limited specific rate of 0.6 d^{-1}, about 40% of the maximum rate in the absence of iron limitation. At this same Fe:C ratio, we estimate that *E. huxleyi* would be able to grow at an iron limited rate of $\sim$0.5 d^{-1}. These predicted rates of 0.5–0.6 d^{-1} fall within the measured range (0.2–0.8 d^{-1}) for specific growth rates of phytoplankton in the subarctic Pacific (Welschmeyer et al., 1991). Our predicted iron-limited rates also agree well with rates observed in algal grow-out incubation experiments conducted during July–August in near-surface water from the same three subarctic Pacific stations where Fe and PO_4 profiles were also taken (see Table 2; Martin et al., 1989). Maximum specific algal growth rates of 0.4–0.8 d^{-1} were observed in the ambient seawater (as based on chlorophyll data), and the addition of 5–10 nM Fe increased rates to 0.9–1.2 d^{-1}, indicating that ambient rates were iron-limited (Martin et al., 1989).

The above findings indicate a basic coherence among the results of our culture experiments, field observations of iron:phosphate regression slopes within oceanic nutriclines (and inferred Fe:C contents of phytoplankton), and observed iron-limited growth rates of the phytoplankton community. This coherence supports the hypothesis that iron distributions within the nutricline are largely controlled by biological uptake and regeneration, as occurs for N, P and Si.

By contrast, there is no apparent coherence between recent measurements of [Fe′] in surface open ocean seawater and values required for growth of oceanic phytoplankton in our experiments. Measurements of iron speciation by cathodic stripping voltammetry indicate that an average of 99.98% of the dissolved iron in surface seawater from the North Pacific is complexed to unidentified strong organic ligands (Rue and Bruland, 1995-this volume). This complexation decreased [Fe(III)′] in the near-surface seawater to 0.01–0.07 pM, well below the value (2 pM) needed to support the growth of *T. oceanica* and *E. huxleyi* at a typical oceanic rate of 0.5 d^{-1}.

At first glance, these results would seem to indicate that diffusion and ligand-exchange of dissolved inorganic Fe(III) species would be insufficient to meet the metabolic demands for growth of oceanic phytoplankton, and that cells would, therefore, need to directly access organically complexed iron. Such direct accessing, for example, might involve uptake of iron–siderophore chelates or reduction of chelated Fe(III) to Fe(II) at the cell surface.

It may be too early, however, to abandon the general model of algal uptake of iron via diffusion of kinetically labile Fe′ species to the cell surface followed by iron transfer from these species to membrane uptake ligands. We note that there is mounting evidence that iron undergoes a dynamic redox cycling in near-surface seawater (Waite and Morel, 1984; Wells and Mayer, 1991). This cycling involves the photoreduction of iron(III)–organic complexes either in solution or on particle surfaces, followed by dissociation of resultant Fe(II)–organic species to form Fe(II)′, reoxidation of Fe(II)′ by H_2O_2 and O_2 to form Fe(III)′, and rechelation of Fe(III)′ (Sunda, 1994). In solar simulator experiments in filtered coastal seawater, such photoredox cycling resulted in steady state Fe(II) concentrations of 1–4% of the total iron (Miller et al., 1995-this volume). Photoredox cycling should also elevate concentrations of Fe(III)′ since the rechelation of Fe(III)′ will be slow at the low 1–2 nM concentrations of strong-iron binding ligands in ocean waters. For example, Rue and Bruland (1995-this volume) determined a kinetic rate constant of 2×10^6 M^{-1} s^{-1} for the reaction of Fe′ with the strong iron-binding ligand in seawater, equal to the theoretically limiting rate constant for water loss from Fe(III)′ species (Hudson and Morel, 1993). At a typical total ligand concentration of 2 nM, this constant would yield a half-life for Fe(III)′ rechelation of 3 min, similar to the measured half life for reoxidation of Fe(II) in coastal seawater (Miller et al., 1995-this volume). Thus, photoredox cycling could elevate Fe(II) and Fe(III)′ to similar levels.

As seen above, the photoredox cycling of iron amounts to a photodissociation of Fe(III)-chelates and serves to elevate steady state concentrations of kinetically labile Fe(II)′ and Fe(III)′ over levels that would exist at equilibrium in the dark. By enhancing Fe′ concentrations, photoredox cycling enhances algal uptake of iron, a result that has been experimen-

tally verified with both synthetic and natural ligands (Anderson and Morel, 1982; Finden et al., 1984) and one that we observe in our own experiments with changing light conditions (e.g. see Exps. 98 and 107, and 106 and 126, Table 1). In seawater, the photodissociation of only a small fraction of natural Fe(III) chelates could lead to a large increase in Fe′ concentrations. For example, at a dissolved iron concentration of 100 pM, the photodissociation of only 2% of the natural dissolved Fe(III) chelates would increase [Fe′] from ~0.01 pM to 2 pM, and provide an adequate [Fe′] to meet the growth demands of oceanic algae (see Fig. 1A,B).

The extent to which photoredox cycling enhances concentrations of kinetically labile, Fe(II)′ and Fe(III)′ species, and the effect of this enhancement on iron uptake by phytoplankton, remain as central unresolved issues in understanding iron availability to phytoplankton in seawater.

5. Conclusions

Our results indicate that surface area normalized iron uptake rates of oceanic and coastal phytoplankton are similar, apparently because all species are transporting iron near the limits dictated by physics and chemistry. Because of the limitation on transport rates, oceanic species have had to reduce either their cell size or their metabolic requirement for iron (or both) in order to grow at the extremely low iron concentrations that occur in the open ocean. Both strategies have come into play: (1) oceanic communities are often dominated by very small phytoplankton cells and (2) our results show that oceanic species have much lower cellular iron requirements for growth than coastal species. Coastal diatoms have high capacities to take up and store iron, which help support high cellular growth rates of these algae during intermittent bloom conditions.

Acknowledgements

We thank Alfred Hanson for iron analyses of culture media, Maria Bondura and Alex Sharp for technical assistance, and Robert Hudson for critical review of the manuscript. This research was funded by grants from the Office of Naval Research.

References

Anderson, M.A. and Morel, F.M.M., 1982. The influence of aqueous iron chemistry on the uptake of iron by the coastal diatom *Thalassiosira weissflogii*. Limnol. Oceanogr., 27: 789–813.

Boyle, E.A., 1977. Determination of copper, nickel, and cadmium in seawater by APDC chelate coprecipitation and flameless atomic absorption spectroscopy. Anal. Chim. Acta, 91: 189–197.

Brand, L.E., 1991. Minimum iron requirements of marine phytoplankton and the implications for biogeochemical control of new production. Limnol. Oceanogr., 36: 1756–1771.

Brand, L.E., Sunda, W.G. and Guillard, R.R.L., 1983. Limitation of marine phytoplankton reproduction rates by zinc, manganese and iron. Limnol. Oceanogr., 28: 1182–1198.

Entsch, B., Sim, R.G. and Hatcher, B.G., 1983. Indications from photosynthetic components that iron is a limiting nutrient in primary producers on coral reefs. Mar. Biol., 73: 17–30.

Falkowski, P.G., Owens, T.G., Ley, A.C. and Mauzerall, D.C., 1981. Effects of growth irradiance levels on the ratio of reaction centers in two species of marine phytoplankton. Plant Physiol., 68: 969–973.

Finden, D.A.S., Tipping, E., Jaworski, G.H.M. and Reynolds, C.S., 1984. Light-induced reduction of natural iron(III) oxide and its relevance to phytoplankton. Nature, 309: 783–784.

Hanson, A.K. and Quinn, J.G., 1983. The distribution of organically complexed copper and nickel in the Middle Atlantic Bight. Can. J. Fish. Aquat. Sci., 40(Suppl. 2): 151–161.

Harrison, G.I. and Morel, F.M.M., 1986. Response of the marine diatom *Thalassiosira weissflogii* to iron stress. Limnol. Oceanogr., 31: 989–997.

Hudson, R.J.M. and Morel, F.M.M., 1989. Distinguishing between extra-and intracellular iron in marine phytoplankton. Limnol. Oceanogr., 34: 113–1120.

Hudson, R.J.M. and Morel, F.M.M., 1990. Iron transport in marine phytoplankton: kinetics of medium and cellular coordination reactions. Limnol. Oceanogr., 35: 1002–1020.

Hudson, R.J.M. and Morel, F.M.M., 1993. Trace metal transport by marine microorganisms: implications of metal coordination kinetics. Deep-Sea Res., 40: 129–151.

Hutchins, D.A., DiTullio, G.R., and Bruland, K.W., 1993. Iron and regenerated production: Evidence for biological iron recycling in two marine environments. Limnol. Oceanogr., 38: 1242–1256.

La Roche, J., Geider, R.J., Graziano, L.M., Murray, H. and Lewis, K., 1993. Induction of specific proteins in eucaryotic algae grown under iron-, phosphorus-, or nitrogen-deficient conditions. J. Phycol., 29: 767–777.

Martin, J.H. and Gordon, R.M., 1988. Northeast Pacific iron distributions in relation to phytoplankton productivity. Deep-Sea Res., 35: 177–196.

Martin, J.H., Gordon, R.M. and Fitzwater, S.E. and Broenkow, W.W., 1989. VERTEX: phytoplankton/iron studies in the Gulf of Alaska. Deep-Sea Res., 36: 649–680.

Martin, J.H., Fitzwater, S.E. and Gordon, R.M., 1990a. Iron deficiency limits phytoplankton growth in Antarctic waters. Global Biogeochem. Cycl., 4: 5–12.

Martin, J.H., Gordon, R.M. and Fitzwater, S.E., 1990b. Iron in Antarctic waters. Nature, 345: 156–158.

Martin, J.H., Gordon, R.M. and Fitzwater, S.E., 1991. The case for iron. Limnol. Oceanogr., 36: 1793–1802.

Martin, J.H., Fitzwater, S.E., Gordon, R.M., Hunter, C.N. and Tanner, S.J., 1993. Iron, primary production and carbon–nitrogen flux studies during the JGOFS North Atlantic bloom experiment. Deep-Sea Res., 40: 115–134.

Martin, J.H. and others, 1994. Testing the iron hypothesis in ecosystems of the equatorial Pacific Ocean. Nature, 371: 123–129.

Miller, C.B., Frost, B.W., Wheeler, P.A., Landry, M.R., Welschmeyer, N. and Powell, T.M., 1991. Ecological dynamics in the subarctic Pacific, a possibly iron-limited ecosystem. Limnol. Oceanogr., 36: 1600–1615.

Miller, W.L., King, D.W., Lin, J. and Kester, D.R., 1995. Photochemical redox cycling of iron in coastal seawater. Mar. Chem., 50: 63–77, this volume.

Morel, F.M.M., Hudson, R.J.M. and Price, N.M., 1991. Limitation of productivity by trace metals in the sea. Limnol. Oceanogr., 36: 1742–1755.

Paschiak, W.J. and Gavis, J., 1974. Transport limitation of nutrient uptake in phytoplankton. Limnol. Oceanogr., 19: 881–888.

Price, N.M., Harrison, G.I., Hering, J.G., Hudson, R.J., Nirel, P.M.V., Palenik, B. and Morel, F.M.M., 1988/1989. Preparation and chemistry of the artificial algal culture medium Aquil. Biol. Oceanogr., 6: 443–461.

Raven, J.A., 1988. The iron and molybdenum use efficiencies of plant growth with different energy, carbon and nitrogen sources. New Phytol., 109: 279–287.

Redfield, A.C., 1934. On the proportions of organic derivatives in seawater and their relation to the composition of plankton. In: R.J. Daniel (Editor), James Johnson Memorial Volume. Liverpool Univ. Press, Liverpool, pp. 177–192.

Redfield, A.C., Ketchum, B.H. and Richards, F.A., 1963. The influence of organisms on the composition of seawater. In: M.N. Hill (Editor), The Sea, 2. Wiley, New York, NY, pp. 26–77.

Rue, E. and Bruland, K.W., 1995. Complexation of iron(III) by natural organic ligands in the central North Pacific determined by a new competitive equilibration/adsorptive cathodic stripping voltammetric method. Mar. Chem., 50: 117–138, this volume.

Sunda, W.G., 1994. Trace metal/phytoplankton interactions in the sea. In: G. Bidoglio and W. Stumm (Editors), Chemistry of Aquatic Systems: Local and Global Perspectives. Kluwer, Dordrecht, pp. 213–247.

Sunda, W.G. and Huntsman, S.A., 1985. Regulation of cellular manganese and manganese transport rates in the unicellular alga *Chlamydomonas*. Limnol. Oceanogr., 30: 71–80.

Sunda, W.G. and Huntsman, S.A., 1986. Relationships among growth rate, cellular manganese concentrations, and manganese transport kinetics in estuarine and oceanic species of the diatom *Thalassiosira*. J. Phycol., 22: 259–270.

Sunda, W.G. and Huntsman, S.A., 1992. Feedback interactions between zinc and phytoplankton in seawater. Limnol. Oceanogr., 37: 25–40.

Sunda, W.G. and Huntsman, S.A., 1995. Regulation of copper concentrations in the ocean's nutricline by phytoplankton uptake and regeneration cycles. Limnol. Oceanogr., 40: 132–137.

Sunda, W.G., Swift, D.G. and Huntsman, S.A., 1991. Low iron requirement for growth in oceanic phytoplankton. Nature, 351: 55–57.

Trick, C.G., 1989. Hydroxymate siderophore production and utilization in by marine eubacteria. Curr. Microbiol., 18: 375–378.

Trick, C.G., Anderson, R.J., Gillam, A. and Harrison, P.J., 1983. Prorocentrin: an extracellular siderophore produced by the marine dinoflagellate *Prorocentrum minimum*. Science, 219: 306–308.

Waite, T.D. and Morel, F.M.M., 1984. Photoreductive dissolution of colloidal iron oxides in natural waters. Environ. Sci. Technol., 18: 860–868.

Wells, M.L. and Mayer, L.M., 1991. The photoconversion of colloidal iron oxyhydroxides in seawater. Deep-Sea Res., 38: 1379–1395.

Welschmeyer, N.A. and Lorenzen, C.J., 1984. Carbon-14 labeling of phytoplankton carbon and chlorophyll a carbon: Determination of specific growth rates. Limnol. Oceanogr., 29: 135–145.

Welschmeyer, N., Goericke, R. Strom, S. and Peterson, W., 1991. Phytoplankton growth and herbivory in the subarctic Pacific: a chemotaxinomic analysis. Limnol. Oceanogr., 36: 1631–1649.

Wood, P.M., 1978. Interchangeable copper and iron proteins in algal photosynthesis. Studies on plastocyanin and cytochrome c-552 in *Chlamydomonas*. Eur. J. Biochem., 87: 9–19.